ADVANCED HEALTHCARE MATERIALS
www.advhealthmat.de

Physical Properties of Implanted Porous Bioscaffolds Regulate Skin Repair: Focusing on Mechanical and Structural Features

*Shumeng Jiang, Sabrina Cloud Li, Chenyu Huang, Barbara Pui Chan, and Yanan Du**

Porous bioscaffolds are applied to facilitate skin repair since the early 1990s, but a perfect regeneration outcome has yet to be achieved. Until now, most efforts have focused on modulating the chemical properties of bioscaffolds, while physical properties are traditionally overlooked. Recent advances in mechanobiology and mechanotherapy have highlighted the importance of biomaterials' physical properties in the regulation of cellular behaviors and regenerative processes. In skin repair, the mechanical and structural features of porous bioscaffolds are two major physical properties that determine therapeutic efficacy. Here, first an overview of natural skin repair with an emphasis on the major biophysically sensitive cell types involved in this multistage process is provided, followed by an introduction of the four roles of bioscaffolds as skin implants. Then, how the mechanical and structural features of bioscaffolds influence these four roles is discussed. The mechanical and structural features of porous bioscaffolds should be tailored to balance the acceleration of wound closure and functional improvements of the repaired skin. This study emphasizes that decoupling and precise control of the mechanical and structural features of bioscaffolds are significant aspects that should be considered in future biomaterial optimization, which can build a foundation to ultimately achieve perfect skin regeneration outcomes.

1. Introduction

Natural skin repair following tissue damage almost never leads to a perfect regeneration outcome that functionally and structurally resembles the original tissue because skin accessories, such as hair follicles,[1] sebaceous glands, and sensory nerves, can barely regenerate in adults. Additionally, certain wound types (e.g., severe burns, diabetic foot ulcer) create a nonhealing microenvironment (e.g., hypoxia and nutritional deficiency) that hinders skin restoration.[2] Therefore, assisted skin repair is needed for augmented skin regeneration in clinical applications.[3] As the most representative accomplishment of regenerative medicine, skin repair using artificially engineered skin substitutes shows great promise in treating severe, medically challenging skin damage with traditional interventions. Since 1997, several artificially engineered skin substitutes (e.g., Dermagraft, Integra, Apligraft, Matriderm, and Hyalomatrix) have been approved by the US Food and Drug Administration (FDA). Among them, several products are based on natural and/or synthetic biomaterial scaffolds (bioscaffolds) that act as a temporary bandage to protect the wound and trigger the formation of new skin tissue. For example, Integra is composed of a top-layered silicon membrane as an epidermis substitute and a bottom-layered collagen–glycosaminoglycan (GAG) scaffold as a dermis substitute.[4] Matriderm acts as a dermal substitute based on collagen and elastin bioscaffolds with porous structures.[5] As a relatively new product, Hyalomatrix, which gained FDA 510k approval in 2007, is a dermal substitute composed of a hyaluronic acid (HA)-derived resorbable bioscaffold.[6] The clinical success of these artificial skin products highlights the significance of implanted biomaterials in skin regeneration.

Implanted biomaterials are generally categorized into hydrogels and porous bioscaffolds. Hydrogel is a class of biomaterials that is characterized by a high water content (>90% of total mass), tiny (<1 μm) pores, and uniformity in structures.[7] Porous bioscaffolds constitute another family of implanted biomaterials with larger pores, usually larger than a single cell. Typical porous bioscaffolds fabricated by the freeze–drying method have round, open pores ranging from 20 to 500 μm.[8] The particle leaching method often produces porous bioscaffolds with pores greater

S. Jiang, S. C. Li, Prof. Y. Du
Department of Biomedical Engineering
School of Medicine
Collaborative Innovation Center for Diagnosis and Treatment of Infectious Diseases
MOE Key Laboratory of Bioorganic Phosphorus Chemistry and Chemical Biology
Tsinghua University
Beijing 100084, China
E-mail: duyanan@tsinghua.edu.cn

Dr. C. Huang
Beijing Tsinghua Changgung Hospital
Tsinghua University
Beijing 102218, China

Prof. B. P. Chan
Tissue Engineering Laboratory
Department of Mechanical Engineering
The University of Hong Kong
Hong Kong, Special Administrative Region, China

DOI: 10.1002/adhm.201700894

than 200 μm,[9] while the pores of electrospun porous bioscaffolds vary from 4 to 100 μm[10] and form between the interconnected fibers.[11] Compared with hydrogels, these interconnected spaces in porous bioscaffolds provide a 3D microenvironment that allows more intensified cellular activities, such as migration and cell–cell interactions. Therefore, porous bioscaffolds are applied to facilitate the regeneration of various tissues, including skin.

To improve regenerative outcomes, most clinically applied bioscaffolds require chemical modifications with bioactive factors such as growth factors (GFs), small molecules, or DNA/RNA fragments. For example, in a rat diabetic wound model, collagen scaffolds bearing vascular endothelial growth factor (VEGF) led to a faster healing rate.[12] Improvements in wound healing have also been achieved with scaffolds modified with various bioactive factors, including b-fibroblast growth factor (b-FGF),[13] thymosin $\beta 4$,[14] and nicotine.[15] These factors facilitate reepithelialization, extracellular matrix (ECM) production and angiogenesis, respectively, for the establishment of a prohealing microenvironment in a wound site. In another example, porous HA scaffolds enriched in nonviral DNA encoding proangiogenic factors have been proven to provide superior clinical outcomes by inducing vascular formation.[16] However, limitations exist for chemically modified bioscaffolds, such as their increasing cost and reduced lifespan caused by accelerated proteolytic degradations (e.g., GF degradation prior to treatment can result in limited efficiency). In addition, uncontrolled release and diffusion of bioactive molecules into peripheral wound tissues may result in undesirable side effects (e.g., excessive fibroblast and ECM accumulation, subsequently leading to potential fibrosis in adjacent tissues if uncontrolled b-FGFs diffuse into peripheral tissues). Therefore, the exploration of alternative approaches to improve the performance of bioscaffolds, especially modification of their physical properties, has emerged as a promising direction in biomaterial development, which is the focus of the current progress report.

Among the numerous physical properties of bioscaffolds, mechanical features have been highlighted in recent advances in mechanobiology and mechanotherapy. Mechanobiology refers to the study of cellular sensations and responses to mechanical microenvironments, such as the stiffness of ECMs in vivo or the stiffness of cell-attached biomaterials in vitro. For instance, mesenchymal stem cells (MSCs) cultured on polyacrylamide (PA) hydrogels show distinctive differentiation patterns into neurons, myoblasts, and osteoblasts in response to variations in gel stiffness ranging from 0.1 to 25 kPa, which correspond to the stiffness of their natural counterparts (i.e., brain, muscle, and bone, respectively).[17] On the other hand, mechanotherapy refers to the process of mechanical force application to promote normal healing or reverse pathogenic processes.[18] Negative pressure wound therapy (NPWT) is one of the most representative mechanotherapy methods; in NPWT, the wound site is sealed and kept under a vacuum. NPWT is effective in removing extracellular fluid, stabilizing the wound environment, and generating contraction of the wound, resulting in accelerated skin repair.[19] Several studies have highlighted the vital roles of mechanical cues in tissue regeneration, specifically in assisted skin repair. For porous bioscaffolds, the mechanical features described here refer to characteristics including but not limited to stiffness, elasticity, the stress-relaxation rate, and stress stiffening effects.

Shumeng Jiang obtained his bachelor's degree in biomedical engineering from Tsinghua University in 2011 and started his master's degree training in Tsinghua University with Prof. Yanan Du in the same year. His research focus has been on the developing advanced strategies to fine-tune physical properties for porous scaffolds as tailored alternatives to natural tissue transplantation in tissue engineering and regenerative medicine.

Sabrina Li obtained a bachelor's degree in science (cell biology and genetics) from the University of British Columbia, Canada, and a master's degree in biomedical engineering from Boston University, US. Prior to taking her Master's degree, she had worked as a research student in the Prostate Center at Vancouver General Hospital. In 2017, she joined Dr. Yanan Du's group in the Department of Biomedical Engineering, School of Medicine, Tsinghua University, for her Ph.D. degree. Her research has been focused on the mechanoactivation of fibroblasts in the context of liver fibrosis using computer-aided simulation.

Yanan Du received a bachelor's degree in chemical engineering from Tsinghua University and a Ph.D. in bioengineering from National University of Singapore. He completed postdoctoral training at Harvard-MIT Division of Health Science and Technology, MIT, and Harvard Medical School. In 2010, he joined the Department of Biomedical Engineering, School of Medicine, Tsinghua University, as an Associate Professor. His research focuses on developing microengineered cell-based assays and therapy platform for drug screening, disease study, and regenerative therapy.

The structural features (e.g., pore structures) of bioscaffolds can also directly influence cellular behaviors such as cell–cell interactions in assisted skin repair,[20] indicating that structural features should be considered in bioscaffold optimization to regulate cell functions in skin repair. For porous bioscaffolds,

the typical structural features include the mean pore size, porosity, organization patterns of the pores, and the surface topography. With the advancement of biomaterials and tissue engineering, numerous bioscaffolds with various mechanical and physical features have been fabricated to facilitate regeneration, which are summarized in **Table 1**.

In this progress report, we will first summarize the physiological skin repair process with a focus on major biophysically sensitive cell types. Then, we will specify the four roles of bioscaffolds as implanted grafts in assisted skin repair. Thereafter, the physical properties of bioscaffolds and their influences on skin repair will be discussed in detail with potential mechanistic insights. Specifically, we will focus on how the mechanical and structural features of porous bioscaffolds regulate skin repair in regenerative therapy.

2. Major Biophysically Sensitive Cell Types Involved in the Four-Stage Skin Repair Process

Natural skin repair involves four essential stages, namely, hemostasis, inflammation, reconstruction, and remodeling.[42] The major cell types involved in these four stages are proven to be biophysically sensitive, highlighting the significant role of biophysical regulation in this regenerative process.

2.1. Hemostasis (Figure 1A)

The initial hemostasis stage is vital for the prevention of blood loss in acute skin damage, but not in chronic damage. Immediately after wounding, vascular rupture and blood cell infiltration occur, initiating coagulation. Coagulation is triggered by platelet activation and fibrin clot formation, eventually leading to hemostasis. Platelet activation is sensitive to the physical properties of the surrounding matrices. In one study, a stiffer fibrinogen substrate could induce stronger platelet adhesion via Rac-1 activation and a larger platelet spreading area via myosin-mediated actin polymerization. Meanwhile, the expression of integrin $\alpha_{IIb}\beta_3$ and P-selectin in platelets is upregulated on stiffer substrates, indicating mechanoresponsive activation.[43] It can be deduced that coagulation speed during skin injury as determined by platelet activation would be sensitive to the physical properties of the lesion site.

2.2. Inflammation (Figure 1B)

The inflammation stage following skin damage usually predominates during the first 2 d. The primary purpose of launching an immune response is to neutralize bacteria, clean out foreign materials, and stimulate neovascularization for subsequent tissue reconstruction. Hemostasis matrices (i.e., a fibrin clot) formed in the former stage serve as natural scaffolds for infiltrating cells and subsequent regeneration. Neutrophils and macrophages are among the first batch of infiltrating cells recruited to the wound site, which predominate during the inflammation process and are well characterized for their functions of removing dead tissues and foreign materials (e.g., bacteria). Moreover, these immune cells, especially macrophages, are responsive to microenvironmental changes in terms of physical properties. For example, macrophage activation toward a pro-inflammatory phenotype is achieved on a polyethylene glycol (PEG)-based 2D hydrogel substrate with a stiffness of 840 kPa compared to its 130 or 240 kPa counterparts.[44] Proinflammatory macrophages express high levels of tumor necrosis factor-α (TNF-α), interlukine-1β (IL-1β), and IL-6 and activate the toll-like receptor 4 (TLR4) signaling pathway, which promotes inflammation in the wound site. This phenomenon has also been proven in a PA hydrogel system in which the production of proinflammatory cytokines, such as TNF-α and IL-1β, by macrophages increases with increasing substrate stiffness from 0.3 to 230 kPa.[45] Once activated, the immune cells release proinflammatory and proangiogenesis cytokines (e.g., IL-6 or VEGF) to promote endothelial cell (ECs) differentiation and vascularization, which is vital for granulation tissue formation in the subsequent reconstruction stage.[46] Vascularization is subject to the regulation of various physical cues, such as the hemodynamic forces produced by constant blood flow, which is required for ECs to maintain their physiological functions (e.g., ion fluxes and endothelial transcription Krüppel-like Factor 2, KLF2, expression).[47] In addition, substrate stiffness has been shown to modulate EC stiffness, adhesion, migration, and proliferation, which are determining factors in angiogenesis,[48] indicating a highly mechanodependent process during angiogenesis.

2.3. Reconstruction (Figure 1C)

The reconstruction stage is characterized by cellular migration and proliferation and the formation of granulation tissue. Migratory fibroblasts and macrophages are recruited to the wound site along with newly formed vasculature to produce granulation tissue, which replaces the fibrin clot.[49] The activated fibroblasts in granulation tissue exhibit myofibroblastic phenotypes with highly expressed α-smooth muscle actin (α-SMA), enhanced contractility, and increased secretion of ECM components (e.g., Collagen I).[50] The presence and proliferation of myofibroblasts allows contraction of the wound edge, which facilitates wound closure. The ECM components secreted by myofibroblasts accumulate and constitute the structural base for dermal tissue reconstruction.[51] Fibroblast activation is conventionally attributed to biochemical factor induction, such as transforming growth factor-β (TGF-β),[52] insulin-like growth factor-1 (IGF-1),[53] and IL-6.[54] More recent advances in mechanobiology provide rich evidence for the mechanical activation of fibroblasts into myofibroblasts when cultured on rigid 2D substrates in the absence of any biochemical induction.[55] In addition, newly formed granulation tissue also serves as a substrate for the migration of other functional cells, such as keratinocytes, which proliferate and mature at the edge of the tissue to restore epithelial function.[56] During reepithelialization, the keratinocytes may be sensitive to physical regulation since the epidermis functions as a physical barrier and a sensor for natural skin tissue. When cultured on PA gels with lower stiffness (i.e., 1.2 kPa), keratinocytes displayed reduced spreading and increased migratory velocities and cell–cell contact (colony formation) compared with those cultured on stiffer

Table 1. Bioscaffolds fabrication with varied mechanical and structural features.

Technique	Reference	Materials	Quantitative characterization of physical properties								Applications/results
			Mechanical features				Structural features				
			Bulk Young's modulus [kPa]	Local Young's modulus [kPa]	Measurement method	Regulation method	Pore size [μm]	Porosity [%]	Pore geometry	Controlling method	
Electro-spinning	[10]	PCL	17.44–21.00	N/A	Tensile test	Fiber thickness	4.66–40.88	65.86–83.22	Irregular, open	Fiber thickness	Electrospun scaffold-based arterial regeneration
	[21]	PCL	N/A	12 000	AFM	N/A	N/A	N/A	Irregular, open	N/A	AFM-based measurement of fiber stiffness
	[22]	Gelatin	N/A	300 000–110 0000	Stimulation based on tensile test	Degree of crosslinking by glucose	N/A	N/A	Irregular, open	N/A	Tensile test combined with theoretical stimulation to characterize the fiber stiffness.
	[23]	Gelatin	2930–4790	N/A	Tensile test	Concentration of gelatin; electrospinning voltage	N/A	N/A	Irregular, open	N/A	The highest tensile modulus of gelatin electrospun scaffold occurs in 7.5% mass concentration of gelatin group
Particle leaching	[24]	PCL	1000–2400	N/A	Compression test	Paraffin particles size	355.5–1229.8	60–70	Closed, round	Paraffin particles size	Increased pore size is beneficial for MSC osteogenesis
	[25]	Collagen	12–21	N/A	Compression test	Ice particles size	150–500	98.8	Open, round	Ice particle size	Increased pore size inhibits in vivo cartilage regeneration
	[26]	PCL	1000–2000	N/A	Compression test	N/A	50–300	75	Open, square	NaCl particle size	New technique to fabricate scaffolds combining salt leaching and wire-network molding.
Freeze–drying	[8]	Tricalcium phosphate (TCP)	1180–2590	N/A	Compression test	Freezing temperature	70–250	55–58	Open, crystal like	Freezing temperature	New technique for tricalcium phosphate scaffold fabrication at different freezing temperatures
	[27]	Collagen	4–7	400–700	Spherical indentation (bulk) AFM (local)	Freezing rate; collagen concentration	70–100	N/A	Open, crystal like	Freezing rate; collagen concentration	The bulk stiffness, but not the local stiffness, can be regulated by collagen concentration
	[28]	Collagen–GAG	N/A	N/A	N/A	N/A	95–151	N/A	Open, crystal like	Freezing temperature	Controlled cooling rates result in more homogeneous pore, while freezing temperature influences the mean pore size
	[29]	Chitin nanowhisker	N/A	N/A	N/A	N/A	N/A	98.3–99.5	Open, aligned	PVA concentrate	New technique for generating aligned pore structure by directional freezing
Gas-foaming	[30]	Gelatin	0.84–4.07	N/A	Tensile test	Degree of crosslinking, polymer density	180–306	N/A	Intercon-nected, bubble-like	Gas pressure, Degree of cross-linking, polymer density,	Four crosslinking agents were applied in scaffold prepara-tion, in which genipin and GTA-crosslinked scaffolds demonstrated higher mechanical strength; genipin also present superior biocompatibility
	[31]	Dextran	N/A	N/A	N/A	N/A	6.0–25.7	80–96	Intercon-nected, bubble-like	Gas volume, concentration of surfactant	New technique for fabrication of highly porous and hydrophilic porous scaffold
Rapid prototyping (3D printing)	[32]	PCL	1900–52 500	N/A	Compression test	Design pattern	245–433	49–57	Open, square/ triangle	Design pattern	New technique to fabricate 3D biodegradable structures with optimal pore size and spatial distribution, providing an adequate mechanical support

Table 1. Continued.

Technique	Reference	Materials	Quantitative characterization of physical properties								Applications/results
			Mechanical features				Structural features				
			Bulk Young's modulus [kPa]	Local Young's modulus [kPa]	Measurement method	Regulation method	Pore size [μm]	Porosity [%]	Pore geometry	Controlling method	
	[33]	Poly(ester urethane)	470–26 300	4780–266 000	Compression test (bulk), compression test of non-porous film (local)	Concentration of polyester triol	423	52.9	Open, square	Design pattern of PCL templates	Angiogenesis, cellular infiltration, collagen deposition, and directional variance of collagen fibers were maximized for wounds implanted with scaffolds having a local stiffness of 24 MPa
Hydrogel (Nonporous)	[34]	Alginate	150–550	N/A	Spherical indentation	Degree of crosslinking, alginate concentration	N/A	N/A	N/A	N/A	Gelation time and Young's modulus are controlled as a function of cation and alginate concentrations
	[35]	Fibrin	1.16–3.85	N/A	Compressive test	Salt (NaCl) concentration	N/A	N/A	N/A	N/A	New technique for rapid fibrin gel fabrication
	[36]	Alginate	N/A	3.6–6.0	AFM	Alginate concentration	N/A	N/A	N/A	N/A	Characterization of the microscale elasticity (local stiffness) of three hydrogels in order to mimic physical properties that the cells experience in vivo
		Fibrinogen/thrombin	N/A	0.5–1.0	AFM	Fibrinogen/thrombin concentration	N/A	N/A	N/A	N/A	
		Hyaluronic acid (HA)	N/A	1.5–2.7	AFM	HA concentration	N/A	N/A	N/A	N/A	
Decellularization	[37]	Porcine adipose	128.57 (tensile strength)	N/A	Tensile test	Tissue type	121.84	89.6%	Physiological structure remained	Tissue type	Decellularized scaffold reseeded with MSCs for promotion of cartilage formation
	[38]	Porcine corneastroma	N/A	N/A	N/A	N/A	16.6–48.5	73.4–82.3%	Physiological structure remained	Freeze temperature	Pore size decreased and porosity increased in acellular porcine cornea stroma fabricated with decreased prefreezing temperature
	[39]	AlloDerm	30 000–70 000	N/A	Tensile test	Tissue type	N/A	N/A	Physiological structure remained	Tissue type	Elastic modulus of acellular dermal matrix as a function of rehydration time
Human skin	[40]	Human skin in vivo	7–8	N/A	Indentation	N/A	N/A	N/A	N/A	N/A	The skin mechanical properties are determined by the subcutaneous layers
	[41]	Human skin ex vivo	420–750	N/A	Tensile test	N/A	N/A	N/A	N/A	N/A	Higher scar grading is synonymous with increased stiffness and decreased extensibility

gels (i.e., 24 kPa),[57] indicating improved coordination for nascent epithelia sheet formation on the softer substrate.

2.4. Remodeling (Figure 1D)

Natural skin repair is finalized during the remodeling stage when the seemingly uniform granulation tissue is remodeled to become well organized and partially functional dermal tissue. After a sufficient amount of ECM accumulates, most myofibroblasts and macrophages in the granulation tissue are programmed to vanish through apoptosis.[58] The cell to ECM ratio decreases together with dynamic changes in the structure and composition of the ECM, transforming immature granulation tissue into mature, functional dermal tissue. In particular, the aligned collagen fibers in the granulation tissue are remodeled and

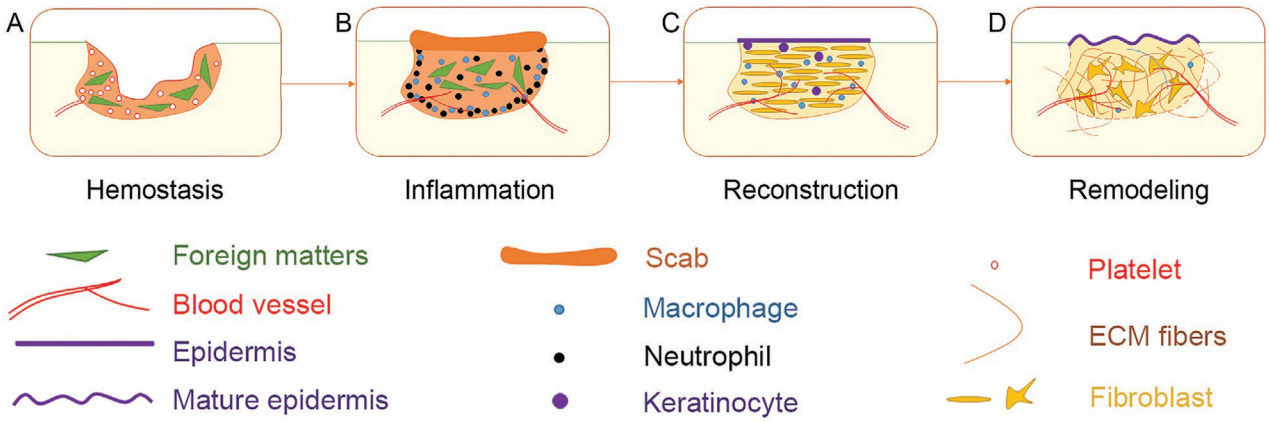

Figure 1. Natural skin repair can be categorized into four stages that involve biophysically sensitive cells. A) The hemostasis stage predominates immediately after skin damage and involves platelet-induced blood clotting. B) The inflammation stage involves initiation of the immune response to remove bacteria and foreign materials and to induce scab formation and neovascularization to create an appropriate prohealing microenvironment. C) The reconstruction stage is characterized by the formation of granulation tissue composed of fibroblasts and macrophages for ECM production. Meanwhile, keratinocytes migrate, proliferate, and differentiate to initiate reepithelialization. D) The remodeling stage, which usually lasts for an extended period, involves ECM deposition and remodeling to form mature dermal tissue with intertwined collagen fibers for mechanical support and a new epidermis. The major cell types involved in skin repair, including platelets, macrophages, fibroblasts, and keratinocytes, are sensitive to physical properties.

reorganized into isotopically distributed collagen fibers, providing sufficient mechanical features in all directions in the matured dermis,[59] while collagen type III is replaced by collagen type I as the predominant ECM component.[60] In the remodeling stage, macrophages polarize into the antiinflammatory phenotype to eliminate unnecessary proinflammatory macrophages and ECM-producing myofibroblasts through the secretion of interleukin-10 (IL-10), which triggers apoptosis. In addition, antiinflammatory macrophages also produce matrix metalloproteinase (MMPs) that breakdown redundant ECM fibers.[61] Studies have demonstrated that insufficient elimination of ECM fibers together with continuous ECM production will eventually result in the formation of a pathological hypertrophic scar.[62] Macrophage polarization toward the antiinflammatory phenotype can be regulated by physical cues in the local tissue microenvironment, including 2D substrate stiffness as described above and also by cell shape alone. In one study, the cell shape of macrophages could be sufficiently controlled using a micropatterning approach, which shows that elongation itself without exogenous cytokine induction can lead to macrophage polarization into an antiinflammatory phenotype.[63]

In conclusion, all major cell types involved in natural skin repair are biophysically sensitive, indicating the significance of physical regulation in homeostasis, inflammation, angiogenesis, proliferation, reepithelialization, and remodeling. The elaborate process of natural skin repair can be disturbed by various conditions, consequently requiring assisted skin repair. In scaffold-assisted skin repair, the implanted bioscaffolds can potentially tune the biophysical sensitivity of cells to control the skin repair process through functions that are worthy of more detailed discussion as below.

3. Four Roles of Porous Bioscaffolds in Assisted Skin repair

The specific roles of bioscaffolds in assisted skin repair have been summarized and categorized into four major aspects: (1) modulation of immune responses; (2) physical support and isolation of the wound area; (3) substitution of natural ECM; and (4) efficient delivery system for cells.

3.1. Modulation of Immune Responses (Figure 2A)

Implanted bioscaffolds induce foreign body responses that mimic the natural immune responses in skin repair to some extent. Taking advantage of these similarities would facilitate the construction of a favorable microenvironment for tissue regeneration. For instance, a prevascularized subcutaneous site can be created by temporary placement of a nylon catheter in mouse models, which can be subsequently removed, supporting diabetes-reversing islet transplantation without the need for a permanent cell-encapsulation device.[64] Such prevascularization process may be partially achieved through the introduction of bioscaffolds to accelerate skin wound healing as well.

The host response toward a biomaterial implant upon injury can be broken down into six stages: blood–material interaction, provisional matrix (PM) formation, acute inflammation, chronic inflammation, formation of granulation tissue/foreign body giant cells, and fibrous encapsulation.[65] Upon blood–material contact, plasma and ECM proteins (e.g., fibrinogen, fibronectin, immunoglobulin G, IgG, and complement fragment iC3b) quickly adsorb onto the bioscaffold interface to gradually form a PM that enables the attachment and migration of inflammatory cells (e.g., macrophages) and fibroblasts through integrin binding.[66] Macrophages assembled at the site of the implant are capable of amplifying the immune response by recruiting more inflammatory cells and inducing angiogenesis via chemokine secretion (e.g., TNF-α).[67] Moreover, as an important constituent of the PM, fibrin has also been found to promote neovascularization around the implant, further validating the causal relationship between the host response and tissue regeneration. Meanwhile, it should be noted that severe foreign body reactions may impede skin repair: fibrous encapsulation

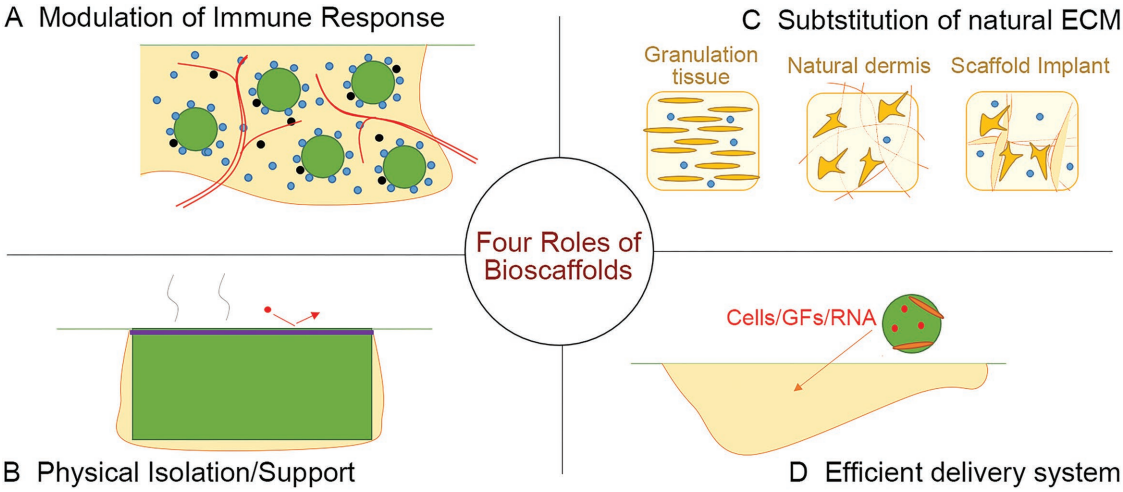

Figure 2. Bioscaffolds have four roles in assisted skin repair. A) Modulation of the immune response contributes to the acceleration of the healing process. B) Physical isolation by bioscaffolds prevents water loss and infection while providing mechanical support to inhibit pathological wound contraction. C) Substitution of natural ECM. The two major differences between newly formed granulation tissue and mature dermis tissue are the structure of the ECM and the amount of each component within the ECM. Natural granulation tissue has a significantly lower ECM to cell ratio compared to the natural dermis, and the majority of its fibrous components are aligned as opposed to disorganized as in its natural counterpart. The application of bioscaffolds with features similar to those of a mature dermis (e.g., collagen accumulation and orientation) could speed up skin repair. D) Bioscaffolds serve as an efficient delivery system for GF, siRNA, cells, and small molecules with controlled and sustained release.

could block the cell–matrix interaction, stop cell infiltration, and prevent blood vessel formation.[68] The benefits and drawbacks of foreign body responses highlight the importance of tailored immune regulation in skin repair.

To elaborate on host immune responses toward implanted bioscaffolds, it is necessary to focus on the polarization of macrophages and their functional modulations in bioscaffold-assisted skin repair. One study demonstrated that a high level of IL-1β expression in proinflammatory macrophages correlates with impaired wound healing in diabetic conditions, but this effect could be reversed through the induction of the VEGF receptor type 1 (VEGFR1) signaling pathway in macrophages.[69] Therefore, it is reasonable to speculate that antiinflammatory macrophages are preferred over the proinflammatory phenotype for skin repair in diabetic patients. A related study showed that an ECM-coated polypropylene mesh could induce macrophage polarization toward the antiinflammatory phenotype in vivo,[70] suggesting that modulation of the macrophage phenotype through the type of bioscaffolds used provides an alternative strategy to regulate the healing process.

The intensity of the host response depends on various features of bioscaffolds, including biocompatibility, surface topology, and the degradation rate. For instance, the fiber size of an electrospun membrane can determine the extent of the macrophage response.[71] Additionally, the faster degradation rate of the polycaprolactone (PCL) scaffold has been associated with improved neovascularization and activation of immune cells that are necessary for skin repair.[72]

3.2. Support and Isolation of the Wound Area (Figure 2B)

Bioscaffolds can provide physical support for the implanted graft while they isolate the wound from the outside environment. Healthy skin naturally exhibits optimal mechanical features that provide protection from external insults. Additionally, the skin forms a physical barrier to prevent potential infections and excessive water loss.[73] Therefore, to design and manufacture bioscaffolds, one should consider these features. In commercialized skin grafts such as Integra, a thin silicon membrane is applied along with collagen–GAG matrices to shield the wound. Apligraft exploits keratinocytes to recreate an artificial epidermis also to achieve shielding effects. Dermal substitutes, such as Matriderm, should be applied along with autologous epidermal grafting for the same purpose. In natural skin repair, scab formation serves to physically protect the wound against further damage. However, naturally formed scabs may be accompanied by undesirable contractions, resulting in the formation of a hypertrophic scar, especially in third-degree burns.[74] Therefore, the application of bioscaffolds may lead to a more stable skin repair process by restricting excessive contractions.

Meanwhile, bioscaffolds should provide sufficient mechanical support while allowing flexibility of the damaged skin. Under natural and unassisted circumstances, damaged skin may be put under compression or stress due to unavoidable bodily movements on a daily basis. In these circumstances, bioscaffolds can stabilize the wound during regeneration. On the other hand, with support from a soft and elastic bioscaffold, the damaged tissue becomes more flexible against routine bodily movements, whereas natural scar tissues are relatively rigid, providing insufficient support for the excessive load introduced by scar contraction or body motions. These mechanical loads on rigid substrates usually lead to ruptures and subsequent secondary injuries. Therefore, bioscaffolds with adjustable flexibility are favorable. It has been validated in a rat model that an adjustable polyurethane composite-based bioscaffold could reduce the risk of secondary injuries, subsequently preventing delayed skin repair.[75] More importantly, bioscaffolds can provide physical support and create spaces for cell migration and proliferation,

allowing cell infiltration into bioscaffolds to produce ECM and GFs to expedite the entire regeneration process.

3.3. Substitution of Natural ECM (Figure 2C)

The involvement of bioscaffolds in ECM remodeling and their integration into living tissues could significantly affect healing outcomes. Unlike the epidermis, the natural dermis mainly acts as a supportive tissue. When the dermal niche is destroyed in pathological conditions, the proliferation and differentiation of implanted dermal cells require the interwoven fibrous networks of bioscaffolds for an equally supportive microenvironment. Most bioscaffolds used for skin repair are composed of organic and biodegradable polymers (e.g., proteins or carbohydrates). These biological polymers are engineered to match the microenvironment, which could possibly trick cells in behave more physiologically.[76] Nevertheless, many questions remain unanswered regarding the applicability of biological polymers, including whether the degradation of protein-based bioscaffolds is controllable, and whether degradation products, particularly proteins, can be recycled to facilitate ECM remodeling.

In addition, intermingled fibrous networks in the natural dermis contribute to the elasticity and tenacity of the skin to some extent. In the granulation tissue formed in the early stage of skin repair, ECM fibers are insufficient alone and are instead aligned in an arrangement.[77] This structural regularity is responsible for suboptimal elasticity and tenacity, preventing the tissue from withstanding dramatic stretching or compression, which could eventually lead to secondary injuries. Porous bioscaffolds, on the other hand, are better substitutes for the natural dermis because the interlaced network gives rise to an open porous network that resembles the mature ECM of the dermis. This delicate network could not only allow free cell infiltration and proliferation to fill the wound, but could also interrupt the formation of aligned ECM fibers and subsequently provide greater elasticity in all directions to facilitate skin repair.

3.4. Efficient Delivery System (Figure 2D)

Bioscaffolds can also serve as a delivery system for both cells and biological agents to further assist regeneration. GFs and stem cells have been widely applied in various clinical regenerative therapies, especially in skin repair. It is generally accepted that IGF-1 promotes reepithelialization,[78] while TGF-β induces fibroblast activation to improve ECM production.[79] However, repetitive injections of GFs for a steady repair process result in high costs, discomfort, and unpleasant clinical experiences. Therefore, skin repair using GFs injections may be limited in clinical applications. Nevertheless, the combination of GFs and bioscaffolds provides an alternative strategy as bioscaffolds can maximally preserve GFs and control their release into a wound.[80] For cell delivery, on the other hand, the effective application of stem cells in skin repair is difficult because most types of wounds are accompanied by severe inflammation and deficiencies in oxygen and nutrients, creating an unfavorable environment for the survival of stem cells.[81] To solve this problem, the in vitro priming of stem cells in porous bioscaffolds before implantation could induce the self-secretion of ECM and GFs and boost stem cell survival in vivo, which could ultimately enhance their therapeutic efficacy.[82]

In summary, the four roles of bioscaffolds in assisting skin repair have been primarily reviewed. The elucidation of these roles and their influences on cell functions would facilitate the exploration of the central question in this report: how the physical properties of bioscaffolds (e.g., mechanical and structural features) influence skin repair through these four roles.

4. How the Mechanical Features of Bioscaffolds Affect Skin Repair

Here, we focus on several key features of bioscaffolds, such as stiffness, elasticity, the stress relaxation rate, and stress stiffening. Each mechanical feature could influence cellular behaviors to some extent and consequently the entire regenerative process. Stiffness, one of the most extensively investigated mechanical features, has been shown to direct cell fate (e.g., MSC differentiation and fibroblast activation) not only in 2D substrates but also in 3D bioscaffolds. It is difficult to determine the stiffness of porous bioscaffolds, which is largely dependent on both their macro- and the microstructures. Each pore within a porous bioscaffold is equivalent to a tiny chamber containing an empty space, which will dramatically reduce the supportive effect provided by the materials and the bulk stiffness of bioscaffolds.[83] Therefore, it can be inferred that local stiffness sensed by the cells is much greater than the bulk stiffness of a bioscaffold. In skin repair, bulk stiffness is mainly considered in terms of its protection and structural support for the entire implant. On the other hand, for cells that are residing within bioscaffolds, whose sizes are usually much smaller than the pores, local stiffness may be the predominant factor regulating their activities.[84] How local stiffness and bulk stiffness synergistically regulate the skin repair process will be explained next based on the four roles of bioscaffolds.

4.1. Modulation of the Immune Response

First, different local stiffnesses of bioscaffolds can trigger various immune responses. A minor modification in the local stiffness could significantly impact the phenotypes and functions of immune cells such as macrophages. It was reported that the activation of proinflammatory macrophages has been found to be positively correlated with substrate stiffness in the former section. In addition, macrophages on a stiffer substrate (i.e., 280 kPa) can generate an increased cell spreading area by nearly eight-fold compared with those on a soft substrate (i.e., 1 kPa).[85] Moreover, the proliferation and migration rates of macrophages are faster on stiff substrates, which can lead to more rapid macrophage recruitment during skin repair (**Figure 3**A). In contrast, in another study based on 3D cultured macrophages on a collagen–GAG scaffold, upregulated antiinflammatory cytokine (e.g., IL-10) expression was correlated with increased matrix stiffness.[86] In addition, a softer bioscaffold can be more easily remodeled by surrounding cellular components, resulting in a more suitable environment

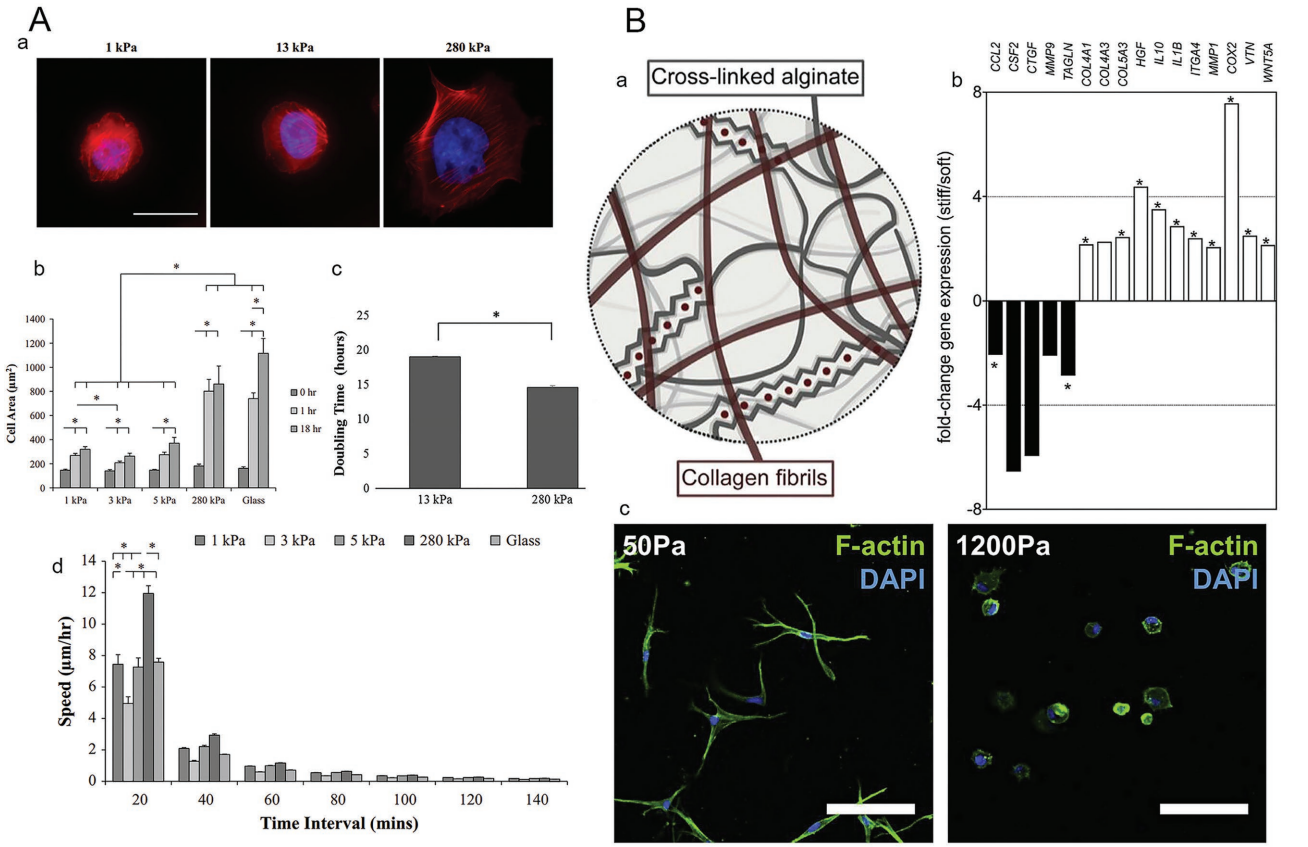

Figure 3. The impacts of the mechanical features of substrates on the in vitro cellular behaviors of macrophages and fibroblasts, which are two of the main biophysically responsive cell types in skin repair. A) The importance of substrate stiffness in regulating macrophages; a) F-actin (red) and nuclear (blue) staining show more organized F-actin and more stress fibers in a stiffer 280 kPa substrate compared to a 1 or 13 kPa substrate. (b) Cell area quantification shows a larger area in a stiffer substrate. c) Doubling time reveals a faster proliferation rate in a stiffer substrate. d) Migration within 20 min reflects the highest rate in the stiffer substrate of 280 kPa. B) The effects of stiffness on dermal fibroblast functions in collagen–alginate bioscaffolds. a) Structural illustration of the collagen–alginate porous bioscaffold and b) gene expression fold changes of the inflammatory mediators IL-10 and Cox2 in response to a stiffness increase from 50 to 1200 Pa. c) The cell morphology changes from a spindle shape on a 50 Pa substrate to a round shape on a 1200 Pa substrate. A) Reproduced with permission.[85] Copyright 2015, European Biophysical Societies' Association. B) Reproduced with permission.[88] Copyright 2014, Elsevier.

for neovascularization and the diffusion of inflammatory and regenerative mediators,[87] suggesting that immune responses and the entire process of skin repair can be modulated through the manipulation of the local stiffness of bioscaffolds.

4.2. Providing Suitable Physical Support

Bioscaffolds with tailored bulk stiffness could provide sufficient protection of the wound while maintaining flexibility to prevent secondary injuries. It has been suggested that precise control of bulk stiffness is required to balance the requirement for sufficient support and flexibility against movements. An increase in bulk stiffness may lead to mechanical tension in the wound area, which may result in scar formation and subsequent restriction in movements with the risk of secondary injuries. For example, in porcine skin repair models, both over-stressed and stress-relaxed skin wounds were established by applying additional external forces and weakening the natural tension, respectively.[89] After 3 weeks, a dramatically higher risk of scar formation was observed in the overstressed wounds compared with that of their stress-relaxed counterparts. A gene array analysis revealed a more proinflammatory tissue phenotype in the over-stressed wounds, which contributed to scar formation. Interestingly, a dramatic decrease in scaffolds' bulk stiffness is not entirely beneficial either since the bioscaffold would be too weak to support the wound against pathological contraction. One study showed that when poly(amidoamine)–poly(*N*-isopropylacrylamide) scaffolds with three different stiffness levels (i.e., ≈200, 1000, and 8000 Pa in 37 °C) were implanted, scar formation was least extensive in the group with medium-stiffness scaffolds (i.e., ≈1000 Pa).[90] Therefore, precise control of the bulk stiffness of bioscaffolds is required to tailor their support, especially the tensile strength in the wound, to achieve satisfactory skin repair.

4.3. Substitution of Natural ECM

The activation of fibroblasts into myofibroblasts during ECM remodeling is highly dependent on the stiffness of adjacent

tissues in vivo and on that of bioscaffolds in vitro. The stiffness of a collagen–alginate scaffold, for instance, can be controlled by manipulating collagen density while the pore structures are maintained by keeping the alginate concentration constant. An analysis of the secretory functions of fibroblasts showed high expression levels of collagen and IL-10 within the 1200 Pa collagen scaffolds compared to those in the softer 50 Pa group (Figure 3B).[88] These data suggest the possibility of modulating fibroblast functions by adjusting bioscaffold stiffness, thereby accelerating ECM accumulation and modulating inflammation.

Meanwhile, macrophages can act as regulatory cells in fibroblast functions, which can be mechanically modulated. One study based on 3D-printed porous scaffolds with different local stiffness levels (i.e., 4.78, 23.9, and 266 MPa) showed interesting results in rat models. Cellular infiltration and proliferation and collagen deposition were maximized in wounds treated with bioscaffolds with a stiffness of 23.9 MPa (**Figure 4**A).[33] This maximization enhanced regenerative response was correlated with increased polarization of macrophages toward a proregenerative phenotype, which was identified through an interlukine-4 (IL-4)-induced macrophage population that secreted IGF-1 and IL-10, thus contributing to the rapid resolution of inflammatory damage.[91]

Moreover, during the remodeling stage, the number of myofibroblasts will eventually decrease when enough ECM has accumulated. In this case, a degradable bioscaffold with a lower local stiffness is preferred during the late stage, which could restrict TGF-β-induced fibroblast activation.[93] Macrophage polarization toward the antiinflammatory phenotype could also be modulated by the local stiffness of bioscaffolds to eliminate myofibroblasts and prevent excessive ECM accumulation through the secretion of MMPs.[94]

4.4. Improving the Delivery Efficiency of Cells and Bioactive Agents

Lastly, controlling the local and bulk stiffness of bioscaffolds could significantly improve the quality and quantity of delivered cells or bioactive agents (e.g., drugs) during therapies. In cell delivery, sufficient attachment to bioscaffolds is required to ensure cell viability. Differences in bioscaffolds' local stiffness may have a significant impact on cell attachment and function.[95]

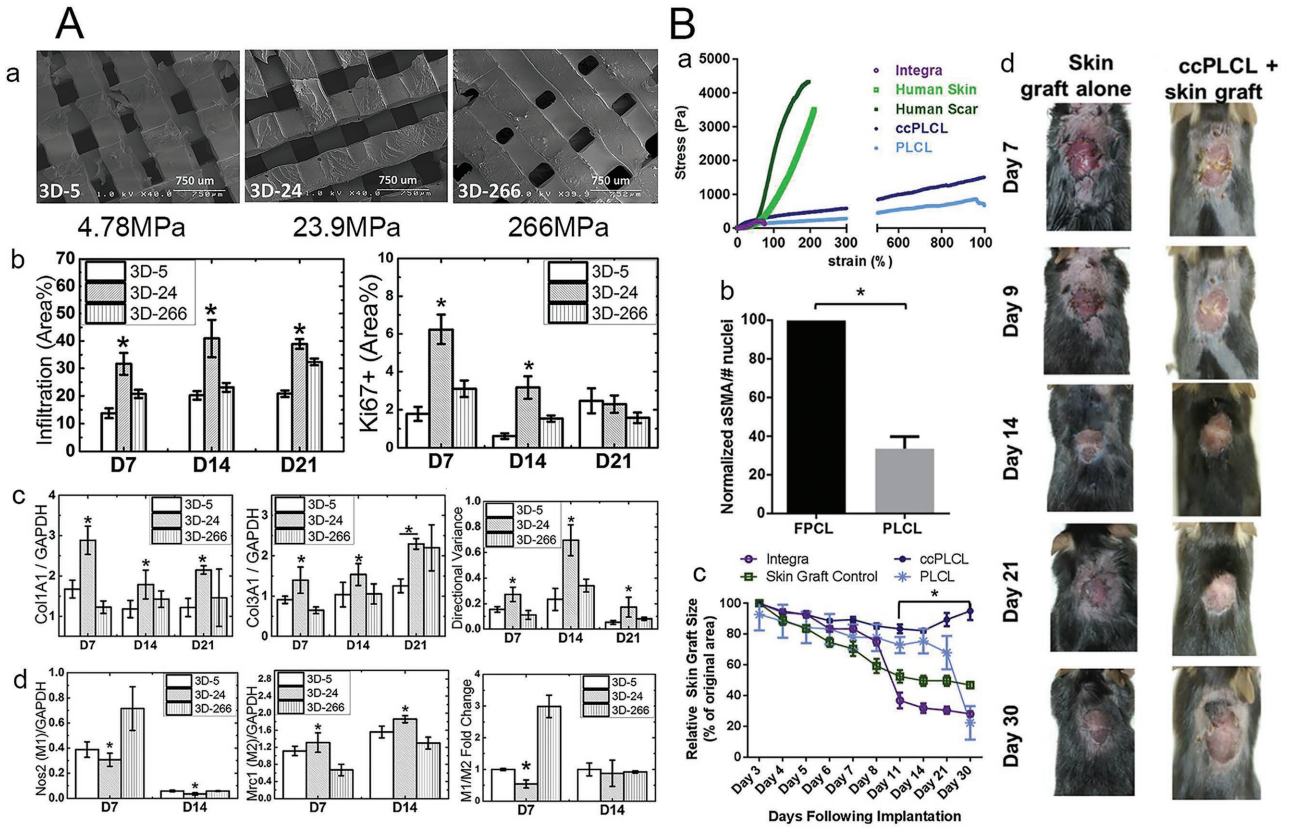

Figure 4. Impacts of mechanical features of bioscaffolds on in vivo skin repair. A) Modulation of the macrophage phenotype and skin repair by controlling the local stiffness of a 3D-printed scaffold in a rat model. a) The 3D-printed scaffolds have variable stiffness levels of 4.78, 23.9, or 266 MPa. The 23.9 MPa scaffold, which resembles natural collagen fibers, shows b) a higher proliferation rate and c) faster ECM production. d) Examinations of the macrophage phenotype show that the greatest proportion of the proregenerative (i.e., M2 in the figure) phenotype among the entire macrophage population is in the 23.9 MPa group. B) An elastomeric and biodegradable collagen-coated PLCL bioscaffold mitigates the effects of hypertrophic scar contraction and alleviates pain. a) PLCL and ccPLCL scaffolds show better elasticity compared to natural human skin. b) Fewer fibroblasts become activated on PLCL scaffolds compared to fibroblast-populated collagen lattice (FPCL) scaffolds and c,d) wounds in mouse models did not show abnormal contraction with the help of the ccPLCL scaffolds beneath the skin graft, preventing the formation of a hypertrophic scar. A) Reproduced with permission.[33] Copyright 2015, Elsevier. B) Reproduced with permission.[92] Copyright 2014, Elsevier.

Moreover, cells can be mechanically primed with a specific local stiffness. Consequently, even after the cells have exited the bioscaffolds and migrated into the damaged tissue, they could carry a "mechanical memory" for specific proliferation and ECM production patterns.[96] Therefore, mechanical priming via local stiffness may potentially augment cell therapy by tuning cellular functions. Additionally, bioscaffolds could serve as cellular carriers for injections due to their protective nature, which primarily depends on bulk stiffness. It has been reported that porous gelatin microscaled bioscaffolds can be microfabricated with low bulk stiffness and high elasticity, allowing them to preserve their structure during injection and protect the cells inside from shear forces. In contrast, hydrogels, which generally exhibit high bulk stiffness, cannot resist shear forces and may break apart during injections, resulting in damage to the inner cells.[97]

The local stiffness of an implanted bioscaffold can also determine bioactive agent (e.g., drug) delivery. It has been reported that by tailoring the Young's modulus (i.e., 24 ± 4 MPa vs 244 ± 22 MPa) of fibers within a PCL/poly(lactic-*co*-glycolic acid) (PLGA) composite electrospun scaffold, one can readily achieve adjustable rates of drug release.[98] Moreover, the release of bioactive agents from bioscaffolds can lead to decreased mechanical properties, as exemplified by the reduced stiffness of tenofovir (TFV)-loaded PCL/PLGA scaffolds post-TFV release. Interestingly, a prestretched PCL/PLGA scaffold showed a higher TFV release rate compared to that of a nonstretched sample,[99] partially due to the reorganization of fibers during the stretching process. In addition to regulation of the release rate, mechanical stimulation can also be applied to trigger biomolecule delivery at a specific time and location. For instance, increased mechanical pressure can be applied to trigger GF (i.e., VEGF) release from alginate hydrogel, thus promoting the regeneration of blood vessels in mouse hindlimb ischemia models.[100]

4.5. Highlights of Other Mechanical Features and Their Influences on Cell Behaviors

Other mechanical features of bioscaffolds, such as stress relaxation, have been primarily investigated in the context of stem cell fate regulation. Stress relaxation refers to the process of the continuous relief of stress when a constant strain is applied to biomaterials. Studies on MSCs have shown that bioscaffolds with a higher relaxation rate could lead to more osteogenesis, but less adipogenesis. In comparison, a stiffer bioscaffold could lead to a similar result, which illustrates the importance of stress relaxation and stiffness in controlling cell fate.[101] Furthermore, stress stiffening is generally defined as the stiffening of biomaterials in response to increased stress. Natural biological fibers, such as F-actin and fibrin, commonly exhibit stress stiffening, whereas widely used synthetic polymeric fibers do not possess this property (e.g., PA fibers). Nevertheless, scientists have developed a variety of catalysts, such as polyisocyanopeptide, that can facilitate the synthesis of biomaterials that exhibit stress-stiffening effects while maintaining unchanged stiffness. Then, cultured MSCs could be induced into the osteogenic lineage accompanied by enhanced runt-related transcription factor 2 (Runx2) expression under a stress-stiffening scaffold.[102] In addition, the elasticity of bioscaffolds may play an important role in preventing pathological contractions at the wound site. A poly(L-lactide-*co*-ε-caprolactone) (PLCL) bioscaffold modified with a layer of collagen on the surface (collagen-coated PLCL, ccPLCL) is more elastic than a natural scar or healthy skin as it allows a greater than tenfold change in a given strain. In the context of skin repair, healed skin does not show dramatic changes in size, which usually result from undesirable contractions (Figure 4B).[92]

4.6. Mechanism of Cellular Mechanosensing of Implanted Bioscaffolds

Despite increasing evidence showing the significant influences of the mechanical features of implanted bioscaffolds on skin repair, the underlying mechanisms remain largely unclear. To achieve mechanical modulation, endogenous cells must interact with implanted bioscaffolds. Nearly all biomaterial implants are subject to the phenomenon of protein adsorption once exposed to blood as the initial host response (**Figure 5**A). The physical linkage between an exogenous implant and endogenous biological components is mainly established through these adsorbed proteins in vivo, which may induce distinctive downstream mechanosensing pathways. Obviously, changes in the surface chemistry of an implant could alter protein

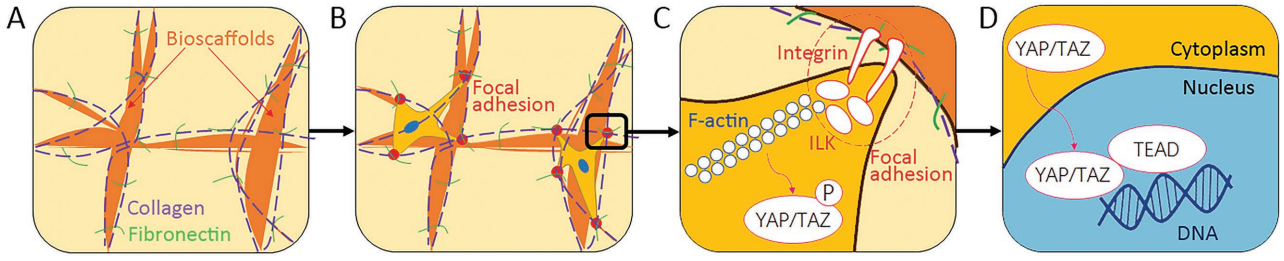

Figure 5. Potential mechanism of cellular mechanosensing of implanted bioscaffolds in skin repair. A) Once implanted, bioscaffolds induce protein adsorption to accumulate ECM proteins on the surface. B,C) The adsorbed proteins enable cell–bioscaffold interactions via integrin, which connects to cytoskeleton F-actin through a focal adhesion (FA) complex. Therefore, differences in the mechanical features of the bioscaffolds can be sensed and transmitted through focal adhesion to the cytoskeleton inside the cells, inducing the activation of transcriptional co-activators (e.g., yes-associated protein/transcriptional coactivator with PDZ-binding motif, YAP/TAZ). D) Activated YAP/TAZ in the nucleus can bind to transcription factors (e.g., transcriptional enhancer activation domain family member, TEAD) to modulate downstream gene expression, cellular function and the efficacy of skin repair.

adsorption, neutrophil activation, and platelet agglomeration.[103] Notably, the composition of adsorbed proteins may reportedly be influenced by physical cues. Fetuin A is one of the proteins that selectively adsorbs onto a stiffer substrate with a much higher affinity compared to a softer substrate. Interestingly, this mechanosensitive protein has also been suggested to improve fibroblast attachment and proliferation on a stiffer substrate.[104] Therefore, it is reasonable to conclude that protein adsorption determines cell–matrix interactions (Figure 5B), and that this adsorption process itself can be influenced by the mechanical features of bioscaffolds.

Upon cell–matrix interaction, local or recruited cells can sense the mechanical cues presented by implanted bioscaffolds through various molecular pathways. Cellular mechanosensing is mainly mediated by the transmembrane receptor integrin family, which provides binding sites for cell adhesion onto bioscaffolds.[105] Integrin binding to bioscaffolds catalyzes the assembly of multiprotein complexes that eventually mature into FAs. Through FAs, mechanical and chemical signals can be intracellularly transduced to regulate many aspects of cell physiology. The size and strength of FAs have been proven to be sensitive to matrix stiffness.[106]

Within FAs, a multifunctional adaptor protein, integrin-linked kinase (Ilk), binds β-integrin cytoplasmic domains and regulates downstream cytoskeleton (i.e., actin microfilament) dynamics by recruiting actin binding regulatory proteins (e.g., α- and β-parvin).[107] Subsequently, changes in the cytoskeleton can regulate downstream signaling, such as the transcription coactivators YAP/TAZ in the Hippo signaling pathway.[108] High levels of F-actin polymerization can promote the nuclear translocation and activation of YAP/TAZ, while depolymerization of F-actin into free G-actin can inhibit YAP/TAZ activation (Figure 5C). Once within the nucleus, YAP/TAZ can interact with DNA-binding transcription factors (e.g., TEAD) to regulate downstream gene expression (e.g., alkaline phosphatase, ALP, expression in MSCs) (Figure 5D).[109] In cells involved in skin repair, YAP/TAZ activation can promote αSMA expression in fibroblasts, resulting in myofibroblast transformation with increased ECM accumulation.[110] Meanwhile, YA/TAZ activation can enhance angiopoietin-2 expression in ECs, which induce endothelial sprouting and angiogenesis.[111] Moreover, CCN1 and CCN2 expression in keratinocytes can also be stimulated by YAP/TAZ to promote keratinocyte proliferation and their ECM (e.g., collagen and fibronectin) secretion. These results highlight the importance of YAP/TAZ signaling in the mechanomodulation of skin repair. In addition to YAP/TAZ, β-catenin in the canonical Wnt receptor signaling pathway has also been shown to mediate downstream mechanotransduction. β-Catenin exists as part of the adherens junctions and is bound to E-cadherin and α-catenin at the cell membrane to interact with the force-generating actin cytoskeleton. Under mechanical stimulation, it translocates to the nucleus and activates the transcription of various Wnt/β-catenin target genes to regulate cellular functions.[112] Interestingly, the time scales of YAP and β-catenin signaling are different. In epithelial cells, nuclear YAP was detected within 1 h of strain application, peaked at 6 h, and then declined rapidly to a background level, while β-catenin was not observed until 6 h after stimulation, but remained for over 24 h.[113]

As a brief summary, during bioscaffold-assisted skin repair, the mechanical features of bioscaffolds are a major concern in material optimization that can be adjusted to fulfill specified regeneration requirements. For porous bioscaffolds, differences between local and bulk stiffness and their potential relationship require further elaboration. It is intuitive to correlate greater local stiffness to greater bulk stiffness, but this may only be true if the microstructures of bioscaffolds remain unchanged. In fact, the microstructures of different porous bioscaffolds can be quite distinctive. For instance, leaching porous bioscaffolds usually have disconnected pores, whereas electrospun porous bioscaffolds usually possess irregular open porous networks. In future investigations, it is necessary to determine how these structural differences influence mechanical features and how they work together to influence skin repair in a synergic fashion. Advances in material science have enabled researchers to fabricate bioscaffolds with microscopic variations in each aspect of their mechanical features, allowing the fine-tuning of cellular behaviors during skin repair.

5. How the Structural Features of Bioscaffolds Affect Skin Repair

3D porous bioscaffolds exhibit excellent structural resemblance to the natural ECM. The structural features (e.g., mean pore size, porosity, and organization pattern of the pores) of porous bioscaffolds can be adjusted accordingly to boost cellular functions in skin repair.[114] The concept of taking advantage of bioscaffolds' structural features to regulate skin repair is relatively new, and only limited research has been conducted to illustrate its efficacy. The current understanding of this concept is mainly based on structural impacts on cellular behaviors in vitro, which show contradictory results as presented in the following sections.

5.1. The Influence of Pore Sizes on Cell behaviors In Vitro

The mean pore size of a bioscaffold is one of the most important parameters known to influence cellular viability, attachment and differentiation.[115] In collagen–GAG scaffolds, dual control of the freezing rate and temperature is used to adjust the mean pore size.[116] In one study, ≈40% of MC3T3-E1 cells attached to bioscaffolds with the smallest pores (100 μm), while less than 20% of cells attached to a 150 μm pore bioscaffold (**Figure 6**A).[28] In contrast, in another study using collagen–GAG scaffolds, a 325 μm pore size was associated with 60% cell attachment, while an 85 μm pore size resulted in only 40% cell attachment (Figure 6B).[117] This preferable cell adhesion to the bioscaffold with larger pores has also been proven using collagen–HA scaffolds with pore sizes ranging from 100 to 300 μm that could be regulated by controlling the crosslinking temperature and the annealing process during freeze–drying.[114] A positive correlation between the percentage of MSC attachment and pore size has been revealed.[118] It is hypothesized that increased ligand density for cell binding and increased surface area are the primary reasons for the enhanced cell adhesion in bioscaffolds with a smaller pore size in the first study. A

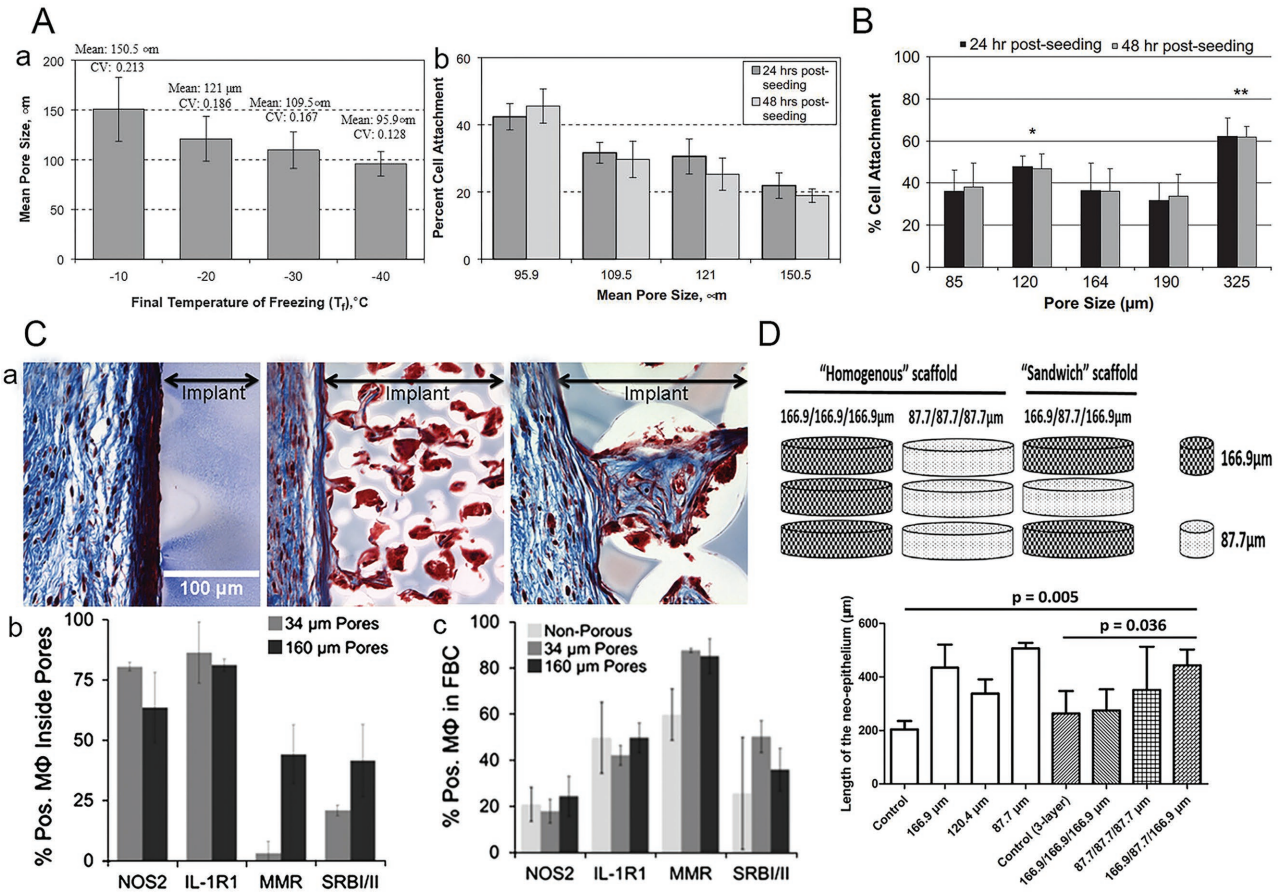

Figure 6. Impacts of the structural features of bioscaffolds on in vitro cellular behavior and in vivo skin repair. A) The mean pore size adjusted by freezing and its influence on cell attachment. a) The long-axis length of pores decreases from 150 to 100 μm as temperature decreases from −10° to −40°. b) The proportion of attached cells decreases as pore size increases. B) In the collagen–glycosaminoglycan scaffold system, the proportion of attached cells increases as pore size increases. C) Pore size affects the magnitude of foreign body reactions in vivo. The ratio between macrophage phenotypes controls the extent of immune responses during the early stage of skin repair. a) The pore size of a bioscaffold is controlled by polymethylmethacrylate particles. The amount and size of pores determine the total area of the scaffold–tissue interface. A nonporous matrix induces the most severe foreign body reaction characterized by the aggregation of nuclei. b) More proregenerative macrophages can be found in bioscaffolds with a pore size of 160 μm than in a 34 μm bioscaffold. c) The macrophages found outside of the bioscaffolds in all three groups show a similar phenotype ratio. D) The spatial orientation of collagen scaffolds with different pore sizes can also influence skin repair. Bioscaffolds with different pore sizes are generated by controlling collagen density. Collagens with different pore size are stacked in different orders to form scaffold sandwiches before application to the wound sites of mice. A hybrid bioscaffold with a small pore size in the middle sandwiched by two layers with a larger pore size resulted in an optimal regenerative outcome. A) Reproduced with permission.[28] Copyright 2004, Elsevier. B) Reproduced with permission.[117] Copyright 2010, Elsevier. C) Reproduced with permission.[120] Copyright 2013, Biomedical Engineering Society. D) Reproduced with permission.[121] Copyright 2015, Acta Biomaterialia.

smaller mean pore size usually correlates with low permeability to soluble factors (e.g., oxygen and nutrients), which could have resulted in malfunctioning cellular activities in the other studies.[119]

This contradictory effect is also evident in the regulation of other essential cellular activities, such as differentiation. For example, the differentiation of MSCs into the chondrogenic lineage was examined in collagen–HA scaffolds with pore sizes ranging from 100 to 300 μm. The largest mean pore size (300 μm) was associated with the highest expression levels of collagen II, glycosaminoglycan and Sox9 and the lowest expression level of collagen I, highly resembling the chondrocyte microenvironment. Meanwhile, the implanted bioscaffolds with a mean pore size of 300 μm were transformed into a stiffer tissue in vivo, eliciting improved chondrocyte regeneration.[118] In another example, the fastest proliferation and calcium accumulation of MSCs in PCL bioscaffolds with different pore sizes (from 400 to 1200 μm) was found in the group with the largest pore size (i.e., 1200 μm) in vitro; the same group also exhibited higher ALP expression and a higher Young's modulus after transplantation.[24] However, a study on collagen-based bioscaffolds demonstrated contradictory results. Ice particles of different sizes were added to a crosslinking solution to produce bioscaffolds with pore sizes ranging from 150–250 to 425–500 μm for primary chondrocyte culture. Better performance with greater collagen II and aggrecan accumulation was achieved in the group with the smallest pores (i.e., 150–250 μm). This result was further supported by a larger Young's modulus and higher

expression levels of collagen II and aggrecan genes in vivo.[25] The pore size of bioscaffolds is clearly an important regulator of cellular behaviors and warrants further attention in future biomaterial developments to resolve the current discrepancies.

5.2. Impacts of Other Structural Features of Bioscaffolds on Cell Behaviors

In addition to pore size, other structural features, such as porosity and the organization pattern of pores, are also important regulators of cell behaviors.

Scaffold porosity refers to the ratio of the hollow space inside a bioscaffold to the overall volume. Therefore, high porosity does not necessarily correspond to a large mean pore size.[122] Studies on scaffold porosity have focused on the regeneration of skeletal tissues. For instance, ceramic scaffolds with porosities varying from 7% to 9% were seeded with stem cells and transplanted subcutaneously into immunodeficient mice. The following evaluations on cell viability and new tissue formation revealed that higher porosity (i.e., 9%) could lead to higher ALP expression and increased scaffold density.[123] These overall changes within the bioscaffold may indicate a more desirable regenerative outcome for new bone tissues. In another case, zirconia was used to synthesize an array of bioscaffolds with porosities ranging from 68% to 93%. Tests on the compressive modulus of these bioscaffolds revealed that higher porosity can lead to greater compressibility, whereas an analysis of cellular behaviors showed that 75% porosity is optimal for cell viability and also corresponds to medium compressive strength for cellular activities.[124] In addition to porosity, the organization pattern (e.g., randomly or aligned) of pores can also be controlled to regulate cell behaviors. Neurons in an electrospun bioscaffold with fibers that were readily arranged in the same direction showed a twofold increase in cell length compared to those in scaffolds with a random fiber orientation.[125] In freeze–dried bioscaffolds, aligned pore structures achieved by the directional freeze–casting technique can be adjusted to fabricate artificial tissues with directional features, such as blood vessels.[29] Considering these structural features (e.g., mean pore size, porosity, and the pattern of pore organization), comprehensive optimization of porous bioscaffolds can be accomplished to precisely regulate various regeneration processes, including skin repair.

5.3. Influences of Bioscaffolds' Structural Features on Skin Repair

Regarding the impacts of bioscaffolds' structural features on skin repair, we first focus on cellular behaviors, especially macrophage polarization. Controlling the macrophage phenotype through the structural modification of bioscaffolds allows researchers to regulate the process of assisted skin repair. A study on electrospun PCL scaffolds illustrated that scaffolds with thicker fibers (i.e., 5–6 μm) and larger pores (i.e., 30 μm) favor macrophage polarization into the proregenerative phenotype, while those cultured in thinner-fiber scaffolds express the proinflammatory phenotype.[10] Apart from macrophage polarization, a study on foreign body reactions provided additional information: a hydrogel devoid of any porous structure was found to induce the most severe foreign body reaction, with enormous amounts of immune cells accumulating around the implanted matrix. However, in bioscaffolds with a mean pore size of 34 or 160 μm, a few macrophages were attracted to the site of the implant. Interestingly, the 34 μm group displayed better angiogenesis and only the 160 μm group showed fibrous tissue deposition in the pores. A larger pore size also results in a macrophage population characterized predominantly by the proregenerative phenotype, while smaller pores are preferred by macrophages of the proinflammatory phenotype (Figure 6C).[120] Therefore, macrophages are obviously sensitive to structural features that may be essential in assisted skin repair.

The direct correlation between pore size and skin repair was demonstrated by a study that used conventional collagen scaffolds with pore sizes of 87.7, 120.4, and 166.9 μm. Within the first 3 d, the rate of wound closure was the same among the three groups. However, the extent of wound closure in the 166.9 μm group appeared to surpass that of the other two groups on day 7, with apparently thicker granulation tissue. In contrast, the cells preferentially deposited the highest amount of ECM, especially collagen fibers, in bioscaffolds with the smallest pore size (87.7 μm). To reconcile this conflict, layer-by-layer blending of the three bioscaffolds with different pore sizes was carried out to achieve a better skin repair outcome. The results showed that the hybrid bioscaffold with a pore size of 87.7 μm in the middle and 166.9 μm on both sides provided the best regenerative outcome. More specifically, this hybrid bioscaffold led to thicker granulation tissue, higher collagen deposition, better reepithelialization, more proliferative cells, and faster wound closure (Figure 6D).[121]

Although the chemical and mechanical features of bioscaffolds have been extensively studied and their functions in assisted skin repair have been uncovered, investigations on how bioscaffolds' structural features influence skin repair are limited. Specifically, the impact of pore size on skin repair is usually difficult to study systematically because methods for precise adjustments of pore size in bioscaffolds are lacking. More efforts should be put forth regarding this important aspect to determine the potential of structural features relative to augmented skin repair.

6. Summary and Discussion

The impacts of bioscaffolds' physical properties on skin repair are the main focus of this progress report. Mechanical features, such as stiffness, have been thoroughly investigated in terms of their potential to generate and modulate immune responses, provide physical support, trigger and control ECM remodeling, and influence the efficacy of substance delivery. Other mechanical features, such as the stress relaxation rate and stress stiffening, have also been found to be important factors. In contrast, the influences of structural features (e.g., pore size, alignment, and porosity) on skin repair have not been sufficiently investigated.

In assisted skin repair, it has been verified that changes in mechanical features, such as stiffness, can trigger suitable inflammation, which may accelerate angiogenesis and activate

fibroblasts to facilitate ECM remodeling and wound contraction, and can ultimately lead to faster wound closure. Meanwhile, structural features, such as the mean pore size, can be controlled to produce optimal skin repair outcomes in the future once the academic community reaches a consensus on the effects of such features. However, challenges remain because the current fabrication methods and controlling approaches are immature, and also because the regulatory mechanisms are not yet clear. In most bioscaffold fabrications, biochemical and physical properties are usually coupled, which means that a change in one could affect the other. Manipulation of collagen density in a collagenous bioscaffold, for example, could simultaneously change the density of adhesion ligands and the stiffness of the bioscaffold. Therefore, it is difficult to determine whether cells adjust their activities in response to changes in stiffness or ligand density. Furthermore, the mechanical and structural features of a specific bioscaffold are not easily controlled independently. For example, the pore size and local stiffness of electrospun bioscaffolds can be manipulated by altering fiber thickness, which would also influence bulk stiffness. For freeze–dried bioscaffolds, although lowering the freezing temperature could lead to a smaller pore size, the degree of cross-linking could also be reduced, resulting in a scaffold with decreased local and bulk stiffness. Meanwhile, comprehensive and standardized characterization approaches are needed to evaluate biophysical properties. Mechanical testing based on tensile force, compression, spherical indentation, or AFM has been applied in most studies to measure the bulk or local stiffness of bioscaffolds, but inconsistencies in testing techniques complicate the evaluation and comparison of bioscaffolds among different studies (Table 1). In addition to image-based analyses, precise and efficient characterization tools for quantitative measurements and information on pore size, shape, distribution, and porosity are lacking. Therefore, mechanical and structural features should be considered synergistically to further optimize bioscaffolds in assisted skin repair and a deeper understanding of the regulatory mechanisms of these features is required. In particular, advanced fabrication techniques and analysis approaches to tailor specific physical properties (e.g., bulk stiffness, local stiffness, pore size, and pore structure) and decoupling of the complex interactions between these properties must be addressed in future research to assist in various wound conditions.

Moreover, variations in the etiology and location of an injury require individual consideration of the properties of each bioscaffold. For instance, a wound in the elbow area, which is constantly moving, may require a bioscaffold with high elasticity to prevent secondary injury. Therefore, the physical properties of a bioscaffold should be tailored for each specific case of skin repair. In addition, the physical microenvironment of a wound is dynamic throughout the healing process, implying that physical properties, such as stiffness, should be made adjustable to satisfy the needs of each healing stage. For instance, while a stiffer bioscaffold may improve ECM accumulation during the reconstruction stage, it may also induce uncontrolled fibroblast activation in the remodeling stage, which could contribute to the formation of a hypertrophic scar. Therefore, it is hypothesized that a degradable bioscaffold with a controlled gradual decrease in stiffness is preferred to maintain the balance between ECM production and fibroblast activation throughout the dynamic repair process. In the future, extensive investigations are required to achieve precise control over the dynamics of bioscaffolds' physical properties and to help us establish strategies for optimal skin repair and regeneration.

Acknowledgements

This work was financially supported by the National Natural Science Foundation of China (Grant Nos. 81522022 and 31671036) and NSFC/RGC Joint Research Scheme (Grant Nos. N_HKU713/14 and 51461165302), and National Key R&D Program of China (Grant No. 2016YFC100810).

Conflict of Interest

The authors declare no conflict of interest.

Keywords

mechanical features, physical properties, porous bioscaffolds, skin repair, structural features

Received: July 27, 2017
Revised: October 23, 2017
Published online: January 15, 2018

[1] J. A. Nowak, L. Polak, H. A. Pasolli, E. Fuchs, *Cell Stem Cell* **2008**, *3*, 33.
[2] M. P. Rowan, L. C. Cancio, E. A. Elster, D. M. Burmeister, L. F. Rose, S. Natesan, R. K. Chan, R. J. Christy, K. K. Chung, *Crit. Care* **2015**, *19*, 243.
[3] S. MacNeil, *Nature* **2007**, *445*, 874.
[4] V. R. Driver, L. A. Lavery, A. M. Reyzelman, T. G. Dutra, C. R. Dove, S. V. Kotsis, H. M. Kim, K. C. Chung, *Wound Repair Regener.* **2015**, *23*, 891.
[5] J. H. Min, I. S. Yun, D. H. Lew, T. S. Roh, W. J. Lee, *Arch. Plast. Surg.* **2014**, *41*, 330.
[6] F. Nicoli, A. Balzani, D. Lazzeri, P. Gentile, R. M. Chilgar, C. Di Pasquali, M. Nicoli, I. Bocchini, A. Agovino, V. Cervelli, *Int. Wound J.* **2015**, *12*, 338.
[7] E. E. Antoine, P. P. Vlachos, M. N. Rylander, *Tissue Eng., Part B* **2014**, *20*, 683.
[8] L. Lin, Z. Wang, L. Zhou, Q. Hu, M. Fang, *Proc. Inst. Mech. Eng., Part H* **2013**, *227*, 50.
[9] Y. Zhao, K. Tan, Y. Zhou, Z. Ye, W. S. Tan, *Mater. Sci. Eng., C* **2016**, *59*, 193.
[10] Z. Wang, Y. Cui, J. Wang, X. Yang, Y. Wu, K. Wang, X. Gao, D. Li, Y. Li, X. L. Zheng, Y. Zhu, D. Kong, Q. Zhao, *Biomaterials* **2014**, *35*, 5700.
[11] M. Abrigo, S. L. McArthur, P. Kingshott, *Macromol. Biosci.* **2014**, *14*, 772.
[12] Q. Tan, B. Chen, X. Yan, Y. Lin, Z. Xiao, X. Hou, J. Dai, *J. Tissue Eng. Regener. Med.* **2014**, *8*, 195.
[13] A. Ayvazyan, N. Morimoto, N. Kanda, S. Takemoto, K. Kawai, Y. Sakamoto, T. Taira, S. Suzuki, *J. Surg. Res.* **2011**, *171*, e247.
[14] D. Ti, H. Hao, L. Xia, C. Tong, J. Liu, L. Dong, S. Xu, Y. Zhao, H. Liu, X. Fu, W. Han, *Tissue Eng., Part A* **2015**, *21*, 541.
[15] P. H. Liem, N. Morimoto, R. Ito, K. Kawai, S. Suzuki, *J. Surg. Res.* **2013**, *182*, 353.

[16] T. Tokatlian, C. Cam, T. Segura, *Adv. Healthcare Mater.* **2015**, *4*, 1084.
[17] A. J. Engler, S. Sen, H. L. Sweeney, D. E. Discher, *Cell* **2006**, *126*, 677.
[18] C. Huang, J. Holfeld, W. Schaden, D. Orgill, R. Ogawa, *Trends Mol. Med.* **2013**, *19*, 555.
[19] C. Huang, T. Leavitt, L. R. Bayer, D. P. Orgill, *Curr. Probl. Surg.* **2014**, *51*, 301.
[20] A. S. Mao, J. W. Shin, D. J. Mooney, *Biomaterials* **2016**, *98*, 184.
[21] S. R. Baker, S. Banerjee, K. Bonin, M. Guthold, *Mater. Sci. Eng., C* **2016**, *59*, 203.
[22] K. Siimon, H. Siimon, M. Jarvekulg, *J. Mater. Sci. Mater. Med.* **2015**, *26*, 5375.
[23] Z.-M. Huang, Y. Z. Zhang, S. Ramakrishna, C. T. Lim, *Polymer* **2004**, *45*, 5361.
[24] P. Y. Huri, B. A. Ozilgen, D. L. Hutton, W. L. Grayson, *Biomed. Mater.* **2014**, *9*, 045003.
[25] Q. Zhang, H. Lu, N. Kawazoe, G. Chen, *Acta Biomater.* **2014**, *10*, 2005.
[26] Y. S. Cho, M. W. Hong, S. Y. Kim, S. J. Lee, J. H. Lee, Y. Y. Kim, Y. S. Cho, *Mater. Sci. Eng., C* **2014**, *45*, 546.
[27] G. S. Offeddu, J. C. Ashworth, R. E. Cameron, M. L. Oyen, *J. Mech. Behav. Biomed. Mater.* **2015**, *42*, 19.
[28] F. J. O'Brien, B. A. Harley, I. V. Yannas, L. J. Gibson, *Biomaterials* **2005**, *26*, 433.
[29] Y. Zhou, S. Fu, Y. Pu, S. Pan, A. J. Ragauskas, *Carbohydr. Polym.* **2014**, *112*, 277.
[30] S. A. Poursamar, A. N. Lehner, M. Azami, S. Ebrahimi-Barough, A. Samadikuchaksaraei, A. P. Antunes, *Mater. Sci. Eng., C* **2016**, *63*, 1.
[31] C. Palocci, A. Barbetta, A. La Grotta, M. Dentini, *Langmuir* **2007**, *23*, 8243.
[32] M. Domingos, F. Intranuovo, T. Russo, R. De Santis, A. Gloria, L. Ambrosio, J. Ciurana, P. Bartolo, *Biofabrication* **2013**, *5*, 045004.
[33] R. Guo, A. R. Merkel, J. A. Sterling, J. M. Davidson, S. A. Guelcher, *Biomaterials* **2015**, *73*, 85.
[34] G. Kaklamani, D. Cheneler, L. M. Grover, M. J. Adams, J. Bowen, *J. Mech. Behav. Biomed. Mater.* **2014**, *36*, 135.
[35] K. C. Murphy, J. K. Leach, *BMC Res. Notes* **2012**, *5*, 423.
[36] C. D. Markert, X. Guo, A. Skardal, Z. Wang, S. Bharadwaj, Y. Zhang, K. Bonin, M. Guthold, *J. Mech. Behav. Biomed. Mater.* **2013**, *27*, 115.
[37] J. S. Choi, B. S. Kim, J. D. Kim, Y. C. Choi, H. Y. Lee, Y. W. Cho, *Tissue Eng., Part A* **2012**, *18*, 80.
[38] J. Xiao, H. Duan, Z. Liu, Z. Wu, Y. Lan, W. Zhang, C. Li, F. Chen, Q. Zhou, X. Wang, J. Huang, Z. Wang, *Biomaterials* **2011**, *32*, 6962.
[39] M. C. Bottino, M. V. Jose, V. Thomas, D. R. Dean, G. M. Janowski, *Dent. Mater.* **2009**, *25*, 1109.
[40] C. Pailler-Mattei, S. Bec, H. Zahouani, *Med. Eng. Phys.* **2008**, *30*, 599.
[41] J. A. Clark, J. C. Y. Cheng, K. S. Leung, *Burns* **1996**, *22*, 443.
[42] G. C. Gurtner, S. Werner, Y. Barrandon, M. T. Longaker, *Nature* **2008**, *453*, 314.
[43] Y. Qiu, A. C. Brown, D. R. Myers, Y. Sakurai, R. G. Mannino, R. Tran, B. Ahn, E. T. Hardy, M. F. Kee, S. Kumar, G. Bao, T. H. Barker, W. A. Lam, *Proc. Natl. Acad. Sci. USA* **2014**, *111*, 14430.
[44] A. K. Blakney, M. D. Swartzlander, S. J. Bryant, *J. Biomed. Mater. Res. A* **2012**, *100*, 1375.
[45] M. L. Previtera, A. Sengupta, *PLoS One* **2015**, *10*, e0145813.
[46] K. V. Eaton, H. L. Yang, C. M. Giachelli, M. Scatena, *Exp. Cell Res.* **2015**, *339*, 300.
[47] P. F. Davies, *Nat. Clin. Pract. Cardiovasc. Med.* **2009**, *6*, 16.
[48] H. Chang, X.-q. Liu, M. Hu, H. Zhang, B.-c. Li, K.-f. Ren, T. Boudou, C. Albiges-Rizo, C. Picart, J. Ji, *Biomacromolecules* **2016**, *17*, 2767.
[49] D. J. Kim, T. Mustoe, R. A. Clark, *Wound Repair Regener.* **2015**, *23*, 318.
[50] S. R. Opalenik, J. M. Davidson, *FASEB J.* **2005**, *19*, 1561.
[51] S. Werner, T. Krieg, H. Smola, *J. Invest. Dermatol.* **2007**, *127*, 998.
[52] D. A. Lanning, R. F. Diegelmann, D. R. Yager, M. L. Wallace, C. E. Bagwell, J. H. Haynes, *J. Pediatr. Surg.* **2000**, *35*, 183.
[53] C. F. Hung, M. G. Rohani, S.-s. Lee, P. Chen, L. M. Schnapp, *Respir. Res.* **2013**, *14*, 102.
[54] V. Doldi, M. Callari, E. Giannoni, F. D'Aiuto, M. Maffezzini, R. Valdagni, P. Chiarugi, P. Gandellini, N. Zaffaroni, *Oncotarget* **2015**, *6*, 31441.
[55] F. Liu, D. Lagares, K. M. Choi, L. Stopfer, A. Marinkovic, V. Vrbanac, C. K. Probst, S. E. Hiemer, T. H. Sisson, J. C. Horowitz, I. O. Rosas, L. E. Fredenburgh, C. Feghali-Bostwick, X. Varelas, A. M. Tager, D. J. Tschumperlin, *Am. J. Physiol.: Lung Cell. Mol. Physiol.* **2015**, *308*, L344.
[56] M. Ben Amar, M. Wu, *J. R. Soc. Interface* **2014**, *11*, 20131038.
[57] H. Zarkoob, S. Bodduluri, S. V. Ponnaluri, J. C. Selby, E. A. Sander, *Cell Mol. Bioeng.* **2015**, *8*, 32.
[58] A. Desmoulière, M. Redard, I. Darby, G. Gabbiani, *Am. J. Pathol.* **1995**, *146*, 56.
[59] K. H. L. Kwan, X. Liu, M. K. T. To, K. W. K. Yeung, C.-m. Ho, K. K. Y. Wong, *Nanomedicine* **2011**, *7*, 497.
[60] H. N. Lovvorn, D. T. Cheung, M. E. Nimni, N. Perelman, J. M. Estes, N. S. Adzick, *J. Pediatr. Surg.* **1999**, *34*, 218.
[61] P. K. Shah, E. Falk, J. J. Badimon, A. Fernandez-Ortiz, A. Mailhac, G. Villareal-Levy, J. T. Fallon, J. Regnstrom, V. Fuster, *Circulation* **1995**, *92*, 1565.
[62] X. Bai, T. He, J. Liu, Y. Wang, L. Fan, K. Tao, J. Shi, C. Tang, L. Su, D. Hu, *Exp. Dermatol.* **2015**, *24*, 355.
[63] F. Y. McWhorter, T. Wang, P. Nguyen, T. Chung, W. F. Liu, *Proc. Natl. Acad. Sci. USA* **2013**, *110*, 17253.
[64] A. R. Pepper, B. Gala-Lopez, R. Pawlick, S. Merani, T. Kin, A. M. Shapiro, *Nat. Biotechnol.* **2015**, *33*, 518.
[65] J. M. Anderson, *Annu. Rev. Mater. Res.* **2001**, *31*, 81.
[66] J. M. Anderson, A. Rodriguez, D. T. Chang, *Semin. Immunol.* **2008**, *20*, 86.
[67] E. L. G. Montrucchio, E. Battaglia, G. Passerin, F. Bussolino, G. Emanuelli, G. Camussi, *J. Exp. Med.* **1994**, *180*, 377.
[68] D. L. Salzmann, L. B. Kleinert, S. S. Berman, S. K. Williams, *Cardiovasc. Pathol.* **1999**, *8*, 63.
[69] S. Okizaki, Y. Ito, K. Hosono, K. Oba, H. Ohkubo, K. Kojo, N. Nishizawa, M. Shibuya, M. Shichiri, M. Majima, *Am. J. Pathol.* **2016**, *186*, 1481.
[70] M. T. Wolf, C. L. Dearth, C. A. Ranallo, S. T. LoPresti, L. E. Carey, K. A. Daly, B. N. Brown, S. F. Badylak, *Biomaterials* **2014**, *35*, 6838.
[71] K. Wang, W.-D. Hou, X. Wang, C. Han, I. Vuletic, N. Su, W.-X. Zhang, Q.-S. Ren, L. Chen, Y. Luo, *Biomaterials* **2016**, *102*, 249.
[72] H. J. Sung, C. Meredith, C. Johnson, Z. S. Galis, *Biomaterials* **2004**, *25*, 5735.
[73] R. Wong, S. Geyer, W. Weninger, J. C. Guimberteau, J. K. Wong, *Exp. Dermatol.* **2016**, *25*, 92.
[74] J. K. Mitsunaga Junior, A. Gragnani, M. L. C. Ramos, L. M. Ferreira, *Acta Cir. Bras.* **2012**, *27*, 417.
[75] E. J. Adolph, A. E. Hafeman, J. M. Davidson, L. B. Nanney, S. A. Guelcher, *J. Biomed. Mater. Res. A* **2012**, *100*, 450.
[76] D. Antoni, H. Burckel, E. Josset, G. Noel, *Int. J. Mol. Sci.* **2015**, *16*, 5517.
[77] A. O. El Sadik, T. A. El Ghamrawy, T. I. Abd El-Galil, *PLoS One* **2015**, *10*, e0137544.
[78] E. Emmerson, L. Campbell, F. C. Davies, N. L. Ross, G. S. Ashcroft, A. Krust, P. Chambon, M. J. Hardman, *J. Invest. Dermatol.* **2012**, *132*, 2838.
[79] H. Chen, W. W. Yang, Q. T. Wen, L. Xu, M. Chen, *Exp. Mol. Pathol.* **2009**, *87*, 189.

[80] M. H. Periayah, A. S. Halim, A. Z. M. Saad, N. S. Yaacob, A. R. Hussein, F. A. Karim, A. H. A. Rashid, Z. Ujang, *Int. J. Clin. Exp. Med.* **2015**, *8*, 15611.
[81] E. Chung, V. Y. Rybalko, P. L. Hsieh, S. L. Leal, M. A. Samano, A. N. Willauer, R. S. Stowers, S. Natesan, D. O. Zamora, R. J. Christy, L. J. Suggs, *Wound Repair Regener.* **2016**, *24*, 810.
[82] Y. Li, W. Liu, F. Liu, Y. Zeng, S. Zuo, S. Feng, C. Qi, B. Wang, X. Yan, A. Khademhosseini, J. Bai, Y. Du, *Proc. Natl. Acad. Sci. USA* **2014**, *111*, 13511.
[83] G. Chen, C. Dong, L. Yang, Y. Lv, *ACS Appl. Mater. Interfaces* **2015**, *7*, 15790.
[84] E. Melo, N. Cardenes, E. Garreta, T. Luque, M. Rojas, D. Navajas, R. Farre, *J. Mech. Behav. Biomed. Mater.* **2014**, *37*, 186.
[85] K. M. Adlerz, H. Aranda-Espinoza, H. N. Hayenga, *Eur. Biophys. J.* **2016**, *45*, 301.
[86] M. Friedemann, L. Kalbitzer, S. Franz, S. Moeller, M. Schnabelrauch, J. C. Simon, T. Pompe, K. Franke, *Adv. Healthcare Mater.* **2017**, *6*, 1600967.
[87] C. Zhou, S. Jin, R. Willing, *Biomech. Model. Mechanobiol.* **2016**, *15*, 1685.
[88] C. Branco da Cunha, D. D. Klumpers, W. A. Li, S. T. Koshy, J. C. Weaver, O. Chaudhuri, P. L. Granja, D. J. Mooney, *Biomaterials* **2014**, *35*, 8927.
[89] M. Januszyk, V. W. Wong, K. A. Bhatt, I. N. Vial, J. Paterno, M. T. Longaker, G. C. Gurtner, *Organogenesis* **2014**, *10*, 186.
[90] S. Chen, J. Shi, X. Xu, J. Ding, W. Zhong, L. Zhang, M. Xing, L. Zhang, *Colloids Surf., B* **2016**, *140*, 574.
[91] F. Chen, Z. Liu, W. Wu, C. Rozo, S. Bowdridge, A. Millman, N. Van Rooijen, J. F. Urban, T. A. Wynn, W. C. Gause, *Nat. Med.* **2012**, *18*, 260.
[92] E. R. Lorden, K. J. Miller, L. Bashirov, M. M. Ibrahim, E. Hammett, Y. Jung, M. A. Medina, A. Rastegarpour, M. A. Selim, K. W. Leong, H. Levinson, *Biomaterials* **2015**, *43*, 61.
[93] Y. Shi, Y. Dong, Y. Duan, X. Jiang, C. Chen, L. Deng, *Mol. Med. Rep.* **2013**, *7*, 419.
[94] M. G. Rohani, R. S. McMahan, M. V. Razumova, A. L. Hertz, M. Cieslewicz, S. H. Pun, M. Regnier, Y. Wang, T. P. Birkland, W. C. Parks, *J. Invest. Dermatol.* **2015**, *135*, 2377.
[95] S. Jalali, M. Tafazzoli-Shadpour, N. Haghighipour, R. Omidvar, F. Safshekan, *Cell Commun. Adhes.* **2015**, *22*, 79.
[96] J. L. Balestrini, S. Chaudhry, V. Sarrazy, A. Koehler, B. Hinz, *Integr. Biol.* **2012**, *4*, 410.
[97] W. Liu, Y. Li, Y. Zeng, X. Zhang, J. Wang, L. Xie, X. Li, Y. Du, *Acta Biomater.* **2014**, *10*, 1864.
[98] D. Carson, Y. Jiang, K. Woodrow, *Pharm. Res.* **2016**, *33*, 125.
[99] S.-F. Chou, K. A. Woodrow, *J. Mech. Behav. Biomed. Mater.* **2017**, *65*, 724.
[100] K. Y. Lee, M. C. Peters, K. W. Anderson, D. J. Mooney, *Nature* **2000**, *408*, 998.
[101] O. Chaudhuri, L. Gu, D. Klumpers, M. Darnell, S. A. Bencherif, J. C. Weaver, N. Huebsch, H. P. Lee, E. Lippens, G. N. Duda, D. J. Mooney, *Nat. Mater.* **2016**, *15*, 326.
[102] R. K. Das, V. Gocheva, R. Hammink, O. F. Zouani, A. E. Rowan, *Nat. Mater.* **2016**, *15*, 318.
[103] I. I. Vlasova, E. V. Mikhalchik, N. A. Barinov, V. A. Kostevich, N. V. Smolina, D. V. Klinov, A. V. Sokolov, *Nanomedicine* **2016**, *12*, 1615.
[104] M. C. Vyner, B. G. Amsden, *Acta Biomater.* **2016**, *31*, 89.
[105] R. O. Hynes, *Cell* **2002**, *110*, 673.
[106] D. Riveline, E. Zamir, N. Q. Balaban, U. S. Schwarz, T. Ishizaki, S. Narumiya, Z. Kam, B. Geiger, A. D. Bershadsky, *J. Cell Biol.* **2001**, *153*, 1175.
[107] a) S. A. Wickström, K. Radovanac, R. Fässler, *Cold Spring Harbor Perspect. Biol.* **2011**, *3*; b) A. Lange, S. A. Wickstrom, M. Jakobson, R. Zent, K. Sainio, R. Fassler, *Nature* **2009**, *461*, 1002.
[108] W. Hong, K.-L. Guan, *Semin. Cell Dev. Biol.* **2012**, *23*, 785.
[109] S. Dupont, L. Morsut, M. Aragona, E. Enzo, S. Giulitti, M. Cordenonsi, F. Zanconato, J. Le Digabel, M. Forcato, S. Bicciato, N. Elvassore, S. Piccolo, *Nature* **2011**, *474*, 179;
[110] F. Liu, D. Lagares, K. M. Choi, L. Stopfer, A. Marinković, V. Vrbanac, C. K. Probst, S. E. Hiemer, T. H. Sisson, J. C. Horowitz, I. O. Rosas, L. E. Fredenburgh, C. Feghali-Bostwick, X. Varelas, A. M. Tager, D. J. Tschumperlin, *Am. J. Physiol.: Lung Cell. Mol. Physiol.* **2015**, *308*, L344.
[111] H.-J. Choi, Y.-G. Kwon, *BMB Rep.* **2015**, *48*, 429.
[112] B. Wang, P. Qin, H. Zhao, T. Xia, J. Wang, L. Liu, L. Zhu, J. Xu, C. Huang, Y. Shi, Y. Du, *Acta Biomater.* **2016**, *41*, 169.
[113] B. W. Benham-Pyle, B. L. Pruitt, W. J. Nelson, *Science* **2015**, *348*, 1024.
[114] M. G. Haugh, C. M. Murphy, F. J. O'Brien, *Tissue Eng., Part C* **2009**, *16*, 887.
[115] I. Bruzauskaite, D. Bironaite, E. Bagdonas, E. Bernotiene, *Cytotechnology* **2016**, *68*, 355.
[116] F. J. O'Brien, B. A. Harley, I. V. Yannas, L. J. Gibson, *Biomaterials* **2004**, *25*, 1077.
[117] C. M. Murphy, M. G. Haugh, F. J. O'Brien, *Biomaterials* **2010**, *31*, 461.
[118] A. Matsiko, J. P. Gleeson, F. J. O'Brien, *Tissue Eng., Part A* **2015**, *21*, 486.
[119] K. L. Crossin, *Cell Adhes. Migr.* **2012**, *6*, 49.
[120] E. M. Sussman, M. C. Halpin, J. Muster, R. T. Moon, B. D. Ratner, *Ann. Biomed. Eng.* **2014**, *42*, 1508.
[121] Y. Wang, R. Xu, G. Luo, Q. Lei, Q. Shu, Z. Yao, H. Li, J. Zhou, J. Tan, S. Yang, R. Zhan, W. He, J. Wu, *Acta Biomater.* **2016**, *30*, 246.
[122] C. S. Rajapakse, M. Bashoor-Zadeh, C. Li, W. Sun, A. C. Wright, F. W. Wehrli, *Radiology* **2015**, *276*, 526.
[123] A. Aarvold, J. O. Smith, E. R. Tayton, S. A. Lanham, J. B. Chaudhuri, I. G. Turner, R. O. Oreffo, *J. Biomed. Mater. Res. A* **2013**, *101*, 3431.
[124] Y. Zhu, R. Zhu, J. Ma, Z. Weng, Y. Wang, X. Shi, Y. Li, X. Yan, Z. Dong, J. Xu, C. Tang, L. Jin, *Biomed. Mater.* **2015**, *10*, 055009.
[125] W. Zhu, F. Masood, J. O'Brien, L. G. Zhang, *Nanomedicine* **2015**, *11*, 693.